Eur. Phys. J. D **9**, 595–599 (1999)

THE EUROPEAN PHYSICAL JOURNAL D

EDP Sciences

Femtosecond dynamics of final-state effects in the valence band photoemission of silver clusters on a graphite substrate

H. Hövel[a], B. Grimm, M. Pollmann, and B. Reihl

University of Dortmund, Experimentelle Physik I, D-44221 Dortmund, Germany

Received: 1 September 1998 / Received in final form: 5 November 1998

Abstract. We studied the electronic structure of quasi size-selected silver clusters grown in nanopits of a graphite surface using ultraviolet photoelectron spectroscopy at $T = 40\,\mathrm{K}$. For clusters with more than 9×10^2 atoms the initial state of the d-electrons has already reached the bulk limit, but there is a dynamic final-state effect which we can explain with a simple model taking into account the finite lifetime of the photohole (corresponding to a charged cluster) and the cluster-substrate interaction on a femtosecond timescale. Below a critical cluster size of about 5×10^2 atoms we have observed additional initial-state effects.

PACS. 36.40.Mr Spectroscopy and geometrical structure of clusters – 79.60.-i Photoemission and photoelectron spectra – 61.16.Ch Scanning probe microscopy: scanning tunneling, atomic force, scanning optical, magnetic force, etc. – 73.23.Ps Other electronic properties of mesoscopic systems

1 Introduction

The investigation of the electronic properties of clusters is largely motivated by one fundamental question: How does the discrete atomic level structure of the atom evolve into the continuous band structure of the bulk? A powerful method to probe the electronic structure of atoms, clusters and the solid state is photoelectron spectroscopy. Therefore it has been applied in many studies concerning the size dependent electronic structure of clusters (e.g. [1–3] and refs. therein). These early studies often used amorphous graphite as a substrate and the cluster production was performed by thermal evaporation. In recent work also well ordered insulating oxide films, metals or semiconductors were used as substrates. A controlled cluster production was achieved, e.g., with the deposition of mass-selected clusters or the cluster growth on nanostructured substrates [4, 5].

There is still a controversy whether the experimental observations of cluster size effects in photoelectron spectroscopy are due to changes in the electronic structure of the clusters i.e. initial-state effects, or caused by the final-state effect originating from the positive charge remaining on the cluster in the photoemission process [1–3]. It has been discussed that this question is strongly influenced by the cluster-substrate interaction [6]. If the substrate is insulating (however preventing a *static* charging, e.g., by the use of a thin film on a conducting substrate) the cluster remains positive during the photoemission process and a shift $\propto e^2/R$, with R the cluster radius, is observed. On a metallic substrate the positive charge is neutralized so fast that no significant shift is observed. Graphite with its semimetallic properties is intermediate between these two extremes and it was suspected that dynamic effects should be visible [6], however, they could not be identified because of limited energy resolution and non-uniform cluster size.

2 Model for a dynamic final-state effect

For the description of the dynamic final-state effect we use a model which takes into account the influence of the photohole remaining on the metal cluster during the photoemission process *and* the cluster-substrate interaction. The charge remaining on the cluster after the photoionization process will cause a shift of the Fermi level. For a free cluster in vacuum, this energy shift describes roughly the difference between the ionization potential of the cluster and the work function of the bulk material. An exact calculation shows this shift is given by $\Delta E = \alpha e^2/(4\pi\varepsilon_0 R)$ with $\alpha = 0.41$ for silver clusters [7]. If one considers the cluster as a small particle of bulk material, the contact with the substrate has to equalize the two Fermi energies. But this is valid only in a static view, since the charge transfer requires some time, depending on the strength of the cluster-surface interaction. For a cluster which is coupled to a substrate the energy shift is time-dependent. It finally vanishes, when an electron is regained from the substrate. For every single cluster this is a quantized process, since the charge amounts to $+e$. The measured energy of the photoelectron depends on how long the positive charge is remaining on the cluster. During this time interval there

[a] e-mail: hoevel@physik.uni-dortmund.de;
Homepage: http://e1.physik.uni-dortmund.de

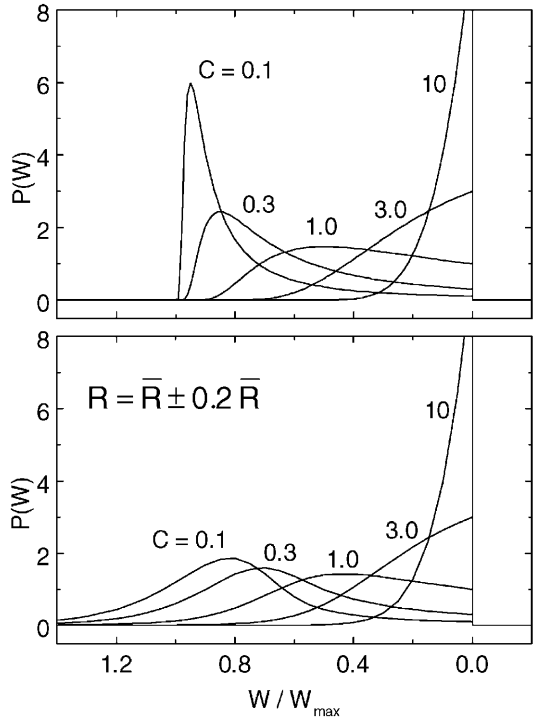

Fig. 1. Top: $P(W)$ calculated with (3) for several values of $C = (R/v\tau)$ assuming clusters identical in radius and coupling to the substrate. Bottom: $P(W)$ calculated assuming a Gaussian size distribution with $R = \bar{R} \pm 0.2\bar{R}$.

is an attractive force reducing the energy. Using a photon energy of 21.2 eV, an electron from the Fermi level is leaving the sample with a kinetic energy of about 17 eV, corresponding to a velocity of $v = 2.4 \times 10^6\,\mathrm{ms}^{-1}$ which is big enough to be sensitive to processes on a femtosecond time scale, because the electron travels a distance corresponding to several cluster radii (of the order of 10^{-9} m) during 10^{-15} s.

In a simple model, the elimination of the positive charge is described by a characteristic time τ which can be interpreted as a tunneling time in the case of a weak cluster-substrate interaction. τ will be dependent on the cluster radius and, additionally, it can vary even for clusters of equal radius owing to a different cluster-substrate coupling. But as a first step we formulate our model for one cluster size and one time τ only. In a second step we will show in which way the results are altered when we include the experimental cluster size distribution. The probability that the charge is eliminated during the time interval $[t, t + \mathrm{d}t]$ is given by

$$P(t)\mathrm{d}t = (1/\tau)\exp(-t/\tau)\mathrm{d}t\,. \tag{1}$$

In order to calculate the energy of the electron arriving at the electron energy analyzer, we need the potential $W(r)$ acting on the electron on its way from the cluster to infinity, with r being the distance from the center of the cluster. A simple formula which fits the limiting cases $W(R) = 0$ and $\lim_{r\to\infty}(\Delta E - W(r)) \propto 1/r$ and should give an estimation of the gross effects is given by

$$W(r) = \frac{\alpha e^2}{4\pi\varepsilon_0}\left(\frac{1}{R} - \frac{1}{r}\right)\,. \tag{2}$$

If the charge on the cluster is neutralized after time t, the energy shift for the electron is equal to $W(R + vt)$. The measured spectra average over a large number of photoelectrons with different times t. This leads – *even if all clusters are identical in radius and coupling to the substrate* – to a distribution of energy shifts given by $P(W)\mathrm{d}W = P(t(W))(\mathrm{d}t/\mathrm{d}W)\mathrm{d}W$ with $W \in [0, W_{\max}]$ and $W_{\max} = \Delta E$. Inserting $W(R + vt)$ one gets with $C = (R/v\tau)$

$$P(W)\mathrm{d}W = \frac{CW_{\max}}{(W_{\max} - W)^2}\exp\left(-\frac{CW}{W_{\max} - W}\right)\mathrm{d}W\,. \tag{3}$$

This function is plotted in Fig. 1 (top) for several values of C, giving the strength of cluster-substrate interaction. For $C \ll 1$ the distribution $P(W)$ approaches a delta function at $W = W_{\max}$ which means that the spectrum is shifted by this amount. This corresponds to the case of free clusters with an infinite lifetime of the photohole. For $C \gg 1$ the photohole is immediately neutralized and $P(W)$ approaches a delta function centered at $W = 0$, i.e. no shift of the spectrum. In the intermediate range, we find curves which cover the interval $[W, W_{\max}]$, giving not only a shift but also a change of the spectral shape. The function $P(W)$ looks similar to the core level line shapes for adsorbates with different coupling-strength to the substrate, studied theoretically [8] as well as experimentally [9]. If the clusters get very small, such a molecular model may also be applicable.

To check on the influence of the cluster size distribution we assumed a Gaussian distribution with $R = \bar{R} \pm 0.2\bar{R}$, which corresponds to the measured cluster sizes in the experiments discussed below. Calculated $P(W)$ curves for the different values of C were summed up with varying $W_{\max}$ according to the size distribution. The results are shown in Fig. 1 (bottom). It is remarkable that the curves for $C > 1$ are almost unchanged by the cluster size distribution, which means the change of the spectral structures is not dominated by averaging over different cluster sizes but by the quantum mechanical size effect which is included in the probability distribution (1) describing that single photoemission processes are characterized by statistically distributed times t.

3 Experimental

The experiments were carried out in the surface-science facility described elsewhere [10]. It combines scanning tunneling microscopy (STM) at $T \leq 5$ K and high-resolution ($\Delta E = 10$ meV) ultraviolet photoelectron spectroscopy (UPS) at $T \leq 50$ K. The clusters were produced by controlled condensation of silver evaporated onto a graphite (HOPG) surface with preformed pits of one monolayer

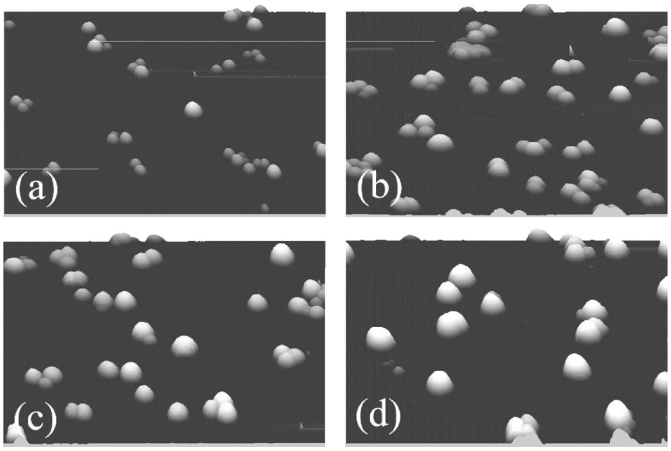

Fig. 2. Topographic STM images (scan area $150 \times 150\,\mathrm{nm}^2$, pseudo 3D display) of silver clusters on graphite (HOPG) produced by controlled condensation in nanopits. Height distributions of (a) 1.8 ± 0.5 nm, (b) 2.4 ± 0.6 nm, (c) 3.1 ± 0.7 nm, and (d) 3.9 ± 0.8 nm; mean number of atoms in one cluster 4×10^2, 9×10^2, 2×10^3, and 4×10^3, respectively.

depth and a diameter of 9 ± 2 nm [5]. Before the silver evaporation was performed in UHV, the nanostructured HOPG surface was heated 1 hour at 870 K, and its cleanliness was checked by UPS. The size distribution of the clusters was determined by the combination of in-situ UHV-STM for the height and ex-situ transmission electron microscopy (TEM) for the lateral diameter. We present results for four different cluster sizes (cf. Fig. 2). The cluster-height distribution as measured with STM was 1.8 ± 0.5 nm, 2.4 ± 0.6 nm, 3.1 ± 0.7 nm, and 3.9 ± 0.8 nm. A diameter-to-height ratio of 1.4 was measured by comparision of TEM and STM data for several samples covering the range of cluster sizes discussed here. With this the mean number of atoms in the clusters are $N = 4 \times 10^2$, 9×10^2, 2×10^3, and 4×10^3, respectively.

The silver clusters produce a distinct signal in the photoemission spectra. By taking the difference curves of the spectra before and after silver evaporation, their spectral contribution could be extracted as described in [10]. In Fig. 3 we present the spectra (taken at $T = 40$ K with $h\nu = 21.2$ eV) of the silver clusters, for the four different cluster sizes of Fig. 2. For comparison we have also measured the analogous spectrum of a thick polycrystalline silver film and show it as the lowest curve in Fig. 3.

4 Discussion

The cluster spectra for the clusters (b)–(d) in Fig. 3 are very similar, but they show distinct deviations compared to the bulk spectrum. We observed that this spectral shape stayed the same even for clusters with $N \approx 3 \times 10^4$ atoms (not shown). The spectrum of the smallest clusters (a) shows much larger differences to the bulk spectrum. We will now use our model for the dynamic final-state effect to analyse these spectra. This implies some simplifications, for example non spherical cluster shapes are not yet included in our model. But this limits essentially only the quantitative interpretation of the parameters C and $W_{\max}$.

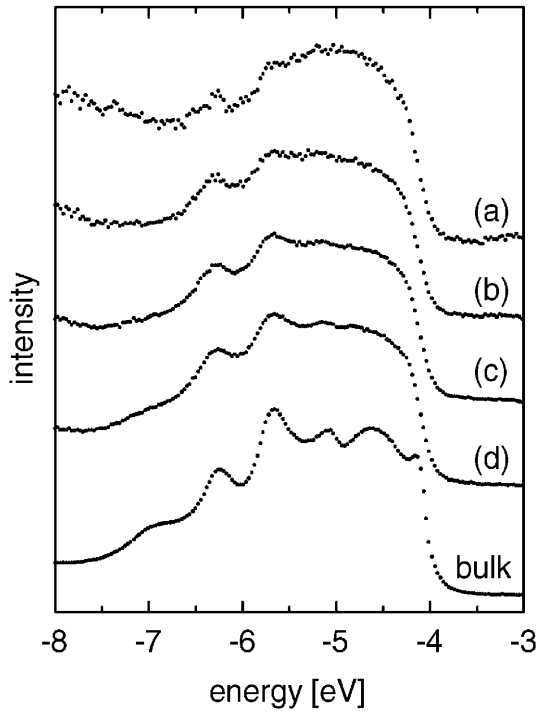

Fig. 3. The spectral contribution of the silver clusters in UPS, measured for the four different samples (a)–(d) of Fig. 2 at $T = 40$ K with $h\nu = 21.2$ eV. The bottom curve was measured for bulk silver with identical parameters. The spectra are normalized to equal height of the valence band structure.

For the clarification of the dynamic final state caused by cluster-substrate interaction it was crucial that we also measured high resolution photoemission spectra of the Fermi level onset [11]. The measured Fermi onset at low temperatures (where the thermal broadening is negligible) is formed by a superposition of sharp Fermi edges shifted with the distribution $P(W)$. For the largest clusters (d) with $N = 4 \times 10^3$ atoms (or, considering the cluster-height distribution explicitly, 2×10^3 atoms to 7×10^3 atoms), the experimental spectrum can be described with the parameters $C = 3.0$ and $W_{\max} = 0.49$ eV (cf. Fig. 4). Together with the mean cluster radius $\bar{R} = 2.5$ nm this results in $\tau = 0.3 \times 10^{-15}$ s which is of the expected order of magnitude for a coupling with significant cluster-substrate interaction as in the case of graphite. The value of $W_{\max} = 0.49$ eV is larger than $\Delta E = 0.24$ eV, the number given in [7] for free silver clusters of the same size. This may be an indication that the cluster-substrate interaction not only provides values $C > 0$, but also changes the total shift given by $W_{\max}$ (cf. [2]). We note that our model of the dynamic final-state effect may be more general in low dimensional metallic systems. For example a similar shape of the Fermi-level onset is observed in UPS of such materials $(TaSe_4)_2I$, $K_{0.3}MoO_3$, $BaVS_3$ and $(TMTSF)_2PF_6^8$ [12].

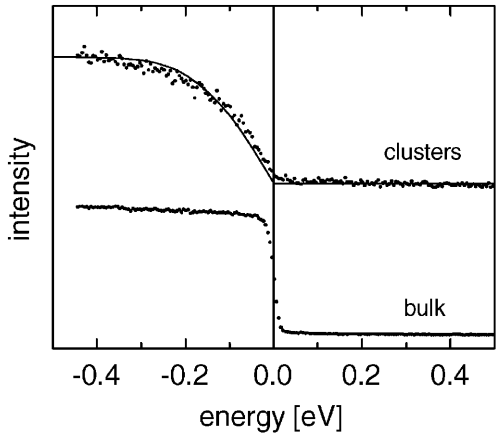

Fig. 4. Top curves: High resolution experimental spectrum of the Fermi-level onset measured at $T = 40\,\mathrm{K}$ for clusters with 4×10^3 atoms (dots) and the spectra calculated using (3) with $C = 3.0$, $W_{\max} = 0.49\,\mathrm{eV}$ and $R = \bar{R} \pm 0.2\bar{R}$ (line). Bottom curve: Fermi-level onset for bulk silver measured with identical parameters.

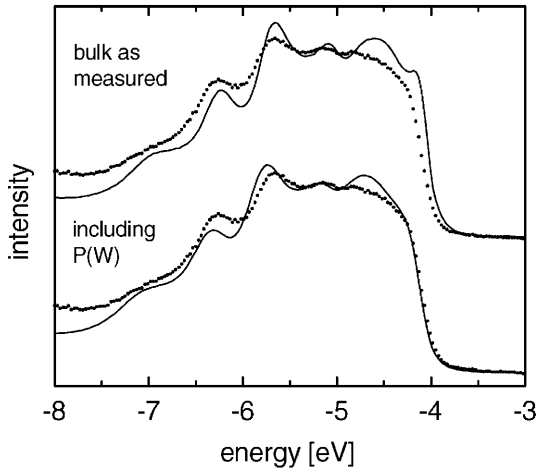

Fig. 5. Dotted curves: The spectral contribution of the silver clusters with 4×10^3 atoms in UPS. Line curves: UPS of bulk silver as measured with identical parameters (top) and convoluted with $P(W)$ with $C = 3.0$, $W_{\max} = 0.49\,\mathrm{eV}$ (bottom).

We can now use these parameters $W_{\max}$ and C and calculate a resulting cluster spectrum by convoluting the measured bulk spectrum with *the same* $P(W)$ as in the case of the Fermi level onset (Fig. 5, bottom). Including only the dynamic final-state effect, we observe that this curve is already very similar to the measured cluster spectrum. Especially the differences in the onset of the d-electrons at $-4\,\mathrm{eV}$ (Fig. 5, top) are correctly removed by this calculation, which is an important fact for the interpretation of optical measurements [13]. The remaining deviations are almost size independent for the clusters (b)–(d) in Fig. 3. The small systematic trend, which we observe in the onset at $-4\,\mathrm{eV}$ (Fig. 3), can be explained with an increase of $W_{\max}$ which corresponds to the variation of the cluster radii $R_d/R_b = 1.6$, however our statistics at the Fermi level onset for the smaller clusters is not good enough for a model fit of $W_{\max}$ and C.

The clusters may have a different crystalline orientation than the polycrystalline bulk sample. This would explain the difference at about $-4.7\,\mathrm{eV}$ (Fig. 5, bottom), where the polycrystalline bulk spectrum shows a peak but bulk Ag(111) has only a small shoulder. We observed with electron diffraction that the silver clusters, which were coagulated in the nanopits at room temperature, do not show such a strong preferential orientation as it was the case for gold clusters grown at 600 °C [14]. But there may be some ordering in correspondence to the (111) orientation, which is observed for silver films on HOPG [15]. Experiments which study the influence of the crystalline structure on the photoemission spectra of clusters are planned.

We conclude that the initial state of the d-electrons for the silver clusters (b)–(d) in Fig. 3 with more than 9×10^2 atoms has already reached the bulk limit (i.e. $R \to \infty$) but there is still a dynamic final-state effect which decreases $\propto 1/R$ and therefore vanishes only very slowly for large clusters. It is especially important to include the dynamic final-state effect in the analysis of UPS of clusters because it results not only in a shift but also alters the shape of the spectra.

For the clusters (a) with $N = 4 \times 10^2$ atoms, however, the initial state seems to be altered in comparison to the bulk limit, because otherwise $R_b/R_a = 1.3$ should give rise to very similar spectra for Fig. 3(a) and (b). This sudden change in the series of cluster sizes (d)–(a) points to a *critical cluster size* of about 5×10^2 atoms for the onset of initial-state effects in the d-electrons of metal clusters. This is in agreement with X-ray photoemission spectra (XPS) [1–3] and data for the optical properties of gold clusters [13]. In the comparison of UPS and XPS spectra one has to consider the influence of the photon energy in $C = (R/v\tau)$. With a typical photon energy of $2 \times 10^3\,\mathrm{eV}$ in XPS a value of $C_{\mathrm{UPS}} = 3.0$ (with $h\nu = 21.2\,\mathrm{eV}$) transforms into $C_{\mathrm{XPS}} = 0.3$, i.e. the photoemission almost fulfills the sudden approximation [16] with the positive charge remaining on the cluster. Indeed this was observed in XPS experiments for silver clusters on amorphous graphite [17].

In order to get a clear separation of initial- and final-state effects for the small clusters it will be important to measure also the shape of the Fermi-level onset for the small clusters (Fig. 2(a)) with good statistics. Such measurements for even smaller clusters are planned.

We thank F. Katzenberg and Professor J. Petermann for taking the TEM pictures and G. Pike and F. Ströwer for their technical assistance with the experiments.

References

1. M.G. Mason, L.J. Gerenser, S.-T. Lee: Phys. Rev. Lett. **39**, 288 (1977); M.G. Mason: in *Cluster Models for Surface and Bulk Phenomena*, NATO-ASI Series B, Vol. 283 (Plenum Press, New York 1992) p. 115
2. G.K. Wertheim, S.B. DiCenzo, S.E. Youngquist: Phys. Rev. Lett. **51**, 2310 (1983)

3. S.B. DiCenzo, G.K. Wertheim: Comments Solid State Phys. **11**, 203 (1985)
4. Y.Q. Cai, A.M. Bradshaw, Q. Guo, D.W. Goodman: Surf. Sci. **399**, L357 (1998); H.-J. Freund: Ang. Chem. Int. Ed. **36**, 452 (1997) and references therein; U. Heiz, F. Vanolli, L. Trento, W.-D. Schneider: Rev. Sci. Instrum. **68**, 1986 (1997); K.H. Meiwes-Broer: Appl. Phys. A **55**, 430 (1992); K. Bromann, H. Brune, Ch. Félix, W. Harbich, R. Monot, J. Buttet, K. Kern: Surf. Sci. **377**–**379**, 1051 (1997)
5. H. Hövel, Th. Becker, A. Bettac, B. Reihl, M. Tschudy, E.J. Williams: J. Appl. Phys. **81**, 154 (1997); H. Brune, M. Giovanni, K. Bromann, K. Kern: Nature **394**, 451 (1998)
6. S.L. Qiu, X. Pan, M. Strongin, P.H. Citrin: Phys. Rev. B **36**, 1292 (1987)
7. M. Seidl, K.-H. Meiwes-Broer, M. Brack: J. Chem. Phys. **95**, 1295 (1991)
8. K. Schönhammer, O. Gunnarsson: Solid State Commun. **23**, 691 (1977)
9. J.C. Fuggle, E. Umbach, D. Menzel, K. Wandelt, C.R. Brundle: Solid State Commun. **27**, 65 (1978)
10. H. Hövel, T. Becker, D. Funnemann, B. Grimm, C. Quitmann, B. Reihl: J. Electron Spectros. Relat. Phenom. **88**–**91**, 1015 (1998)
11. H. Hövel, B. Grimm, M. Pollmann, B. Reihl: Phys. Rev. Lett. **81**, 4608 (1998)
12. B. Dardel, D. Malterre, M. Grioni, P. Weibel, Y. Baer, F. Lévy: Phys. Rev. Lett. **67**, 3144 (1991); M. Grioni, D. Malterre, Y. Baer: J. Low Temp. Phys. **99**, 195 (1995)
13. U. Kreibig: in *Growth and Properties of Metal Clusters*, ed. by J. Bourdon (Elsevier, New York 1980) p. 371
14. H. Hövel, Th. Becker, A. Bettac, B. Reihl, M. Tschudy, E.J. Williams: Appl. Surf. Sci. **115**, 124 (1997)
15. F. Patthey, W.-D. Schneider: Phys. Rev. B **50**, 17 560 (1994)
16. J.W. Gadzuk, M. Sunjic: Phys. Rev. B **12**, 524 (1975)
17. G.K. Wertheim, S.B. DiCenzo, D.N.E. Buchanan: Phys. Rev. B **33**, 5384 (1986)